

# Change of Single Stiffness for Cylindrical Gears with External Involute Teeth: Analytical and FE Determination

Amiya Kumar Biswal<sup>1\*</sup>, Soma Dalbehera<sup>2</sup>

<sup>1\*</sup> Assistant Professor, Department of Mechanical Engineering, Nalanda Institute of Technology, Bhubaneswar, Odisha, India

<sup>2</sup> Associate Professor, Department of Mechanical Engineering, Nalanda Institute of Technology, Bhubaneswar, Odisha, India

\*Corresponding author e-mail: amiyabiswal@thenalanda.com

## **ABSTRACT**

To accurately determine the contact characteristics of tooth pairs, the mesh stiffness must be calculated. The so-called individual stiffness is the simplest estimate of the relative stiffness of the basic profile geometries. Standardized and analytical methods are used to calculate the individual and mesh stiffness of the gears to achieve the design goals, taking into account the load capacity and vibration excited characteristics. These techniques include the Weber and Banaschek equations based on mechanical calculations and the ISO 6336-1:2006 formulas based on experimental relationships. This study provides recommendations to improve analytical calculations. Our goal is to show how variations in applied compression angle, modulus, load, edge thickness and number of teeth affect the maximum stiffness of a person. Our MATLAB program generates the profile shape of the gears. Tool geometry and production kinematics are used to calculate the tool profile. Abaqus accepts imported geometry. The sensitivity of the models to various parameters is investigated and compared with the results of analytical calculations. Two of the most popular analytical calculation techniques in Europe, such as the ISO 6336-1:2006 formulas and the Weber and Banaschek equations, serve as benchmarks for individual stiffness. Keywords cylindrical gear, spiral teeth, single stiffness, FEM, ISO 6336-1:2006, Weber-Banaschek

## **1. Introduction**

Precision power applications require gears that meet a number of technical requirements for both their load capacity and vibration excitation characteristics. To achieve the expected results, it is important to correctly consider the mesh stiffness of the gears. The individual stiffness is the main input to the calculations. When designing gear motors, the load distribution characteristic in the width of the tooth surface and between the teeth is crucial. The stiffness of the web in the specified mounting position is essential for the accurate calculation of bond stresses. It is defined by one basic quantity called contact stiffness. A single stiffness parameter expresses the force required to deform one or more pairs of inflexible teeth contacting a surface width of 1 mm x 1 mm. A more precise definition of single tooth stiffness is needed to assess the degree of vibration excitation. Due to the prevalence of these calculations, their importance has increased significantly. cars electric drives. The aim is to predict the likelihood of likely acoustic problems before using the velocity models. The two main classes of analysis methods currently available are analytical contact analysis and standard approaches that combine basic mathematical operations [1]. The second, often based on the deformation calculation published by Weber and Banaschek (WB) [2], uses a much more sophisticated mathematical solution to describe the individual stiffness. Using this solution, bond stiffness can be determined directly from point to point. Simple strain models are used to determine WB formulas. Lutz's description [3] of the modification of the worm gear deformation calculation method refers to the plane stress model. It should be emphasized that the determination of a single stiffness is not sufficient for analytical modeling of joint tissue stiffness. Several methods can be used to configure the load distribution across a cross section. The computation presented by Kagawa [4] and Hayashi [5] and integrated with the WB [2] method by Schmidt [6] is one of the most used techniques. In [7, 8], new findings regarding analytical computations are presented. The computation method is contrasted in [7] with those used by Fernández et al. [9] and Chen and Shao [10]. Gerber [11] presents the calculation of dynamic forces during the connection. These forces and the stiffness of the mesh are influenced by the geometry that is being used, the torques and speeds, the lubricating properties, the state of the contacting surfaces, etc. The influence of the peeling on the mesh stiffness is discussed in [12, 13]. The effect of the spalling on the friction characteristics can be seen in Saxena et al.'s research [14]. The results reveal the influence of spalling location, size

and shape. He et al. [15] dealt with the theoretical approximation of contact friction and its correlation with measurement results.

In [15], the authors gave the correlation analysis applying as a benchmark the Rebbeschi et al.'s work [16]. The determination of damping of the lubricated gear connection can be found in [17]. The impact of additional geometric errors on the system is also deserved attention. Zhang et al. [18] looked at the dynamic impact of the eccentricity of helical gears and the rotor's imbalance. Results on the impact of eccentricity and profile variations were also provided by Wang and Zhang [19]. The use of FE simulations and hybrid techniques that combine analytical and FEM solutions, which may be categorised into three main classes, is another option for determining the single stiffness. These simulations are dynamic [20–23], quasi-dynamic [24–27], and quasi-static [25–27]. Both two-dimensional and three-dimensional models can be used, depending on the goal of the tests; for examples, see the works [21, 22]. Our study falls under the category of quasi-static calculations because the majority of analytical techniques are utilised to approximate this case. Similar study may be found, for instance, in the works of Hwang et al. [25] and Zhan et al. [27], who used conventional AGMA 2001-D04 using quasi-static models to investigate the association between emerging contact pressure and tooth bending stress. By contrasting the results with the analytical solution outlined by Ziegler's approach [29], Wanderer's work [28] uses the finite element method to illustrate the interaction effect between the teeth pairs in the contact on the single and mesh stiffness. While these calculations should always be done continuously, monitoring the stresses at stiffness calculations is particularly helpful for examining the models' proper settings. offer convergent absolute values for appropriate setting-ups. The outcomes of maximum single stiffness calculation methods, however, cannot be contrasted in terms of their absolute values. The hubs' deformation is the primary cause of the deviation [30–32]. As a result, the results are assessed as the impact of changing various geometric parameters on a single stiffness. [33] discusses how hubs affect tooth deflections. The gear designing process greatly benefits from the effect analysis of each geometric parameter. This can make choosing an appropriate design much easier. The series of studies conducted by Li [26] on the impact of the addendum factor on contact pressure, tooth bending stress, and mesh stiffness serve as an excellent illustration of this. This study presents the sensitivity of the maximum single stiffness to various parameters. Analytical solutions and the outcomes of finite element modelling are also contrasted. Analytical data obtained in accordance with ISO 6336-1:2006 [1] and Weber and Banaschek [2] are used as benchmarks in these tests. Finite element models' boundary conditions are established using analytical techniques. This study emphasises the value of taking hub geometry into account. Our goal is to illustrate the correlation of the sensitivity of the parameter at various rim thicknesses rather than to attempt to match analytical conclusions as closely as feasible. In contrast to the ISO calculations and Weber and Banaschek calculations, the entire hub geometry is taken into account in this article. So, the study approaches the subject from a certain angle.

## 2. Profile geometry and load settings

There are several options for selecting the test version to analyze the effect of the applied geometry. The goal is to identify as comprehensive and clear-cut a series of experiments as possible. In consequence, the geometry of the meshing gears is always identical in the calculations and the single stiffness of the meshing is always evaluated in the pitch point on contact path. This definition means the comparison of the maximum single stiffness because the paired gears will show their maximum or from this slightly different stiffness in the applied load position. The analytical determination of single stiffness of helical gear pairs can be traced back to spur gear pairs. This approximation applies to both the formulas of ISO 6336-1:2006 [1] and the equations of WB method [2]. The current calculations are also based on this approach. As a result, the value of the helix angle is always  $0^\circ$ . Perhaps one of the most obvious parameters of the contact profiles is the pressure angle. Therefore first, the effect of the pressure angle used will be evaluated. The range between  $15^\circ$  and  $25^\circ$  which is the most important in practice has been selected for the analysis. In addition to the effect of the choice of pressure angle on the single stiffness, it is also worth examining its dependence on the normal module. The tests will be carried out on gears with 1 to 5 normal modules. This investigation is especially interesting because the method used by the ISO standard ignores the effect of this parameter. WB method already takes into account the effect of this factor. The negligibility of the load dependence of single stiffness, as in the case of the normal module, is also worth examining separately. The ISO standard considers single stiffness to be a linear function of the load if the tangential force is less than 100 N/mm, while over 100 N/mm it considers it independent. In the case of WB method, there is no simplified consideration in the effect of the load [1]. In

our investigations we shall analyze the 100 N/mm minimum load range. It should be noted that although the ISO standard defines the criterion for the load dependence for tangential force, the single stiffness is calculated according to the definition using the normal force. However, since the normal load is the function of the pressure angle, the tendency of the single stiffness change is plotted as a function of the tangential force. The ISO standard defines the 300 N/mm tangential load as the base case for the formulation of the formulas. Therefore, this load case will be chosen also in this work as reference [1]. The next analyzed issue is the effect of the tooth number on the change of single stiffness. A range of tooth numbers between 35 and 105 was selected to the calculations. The gear ratio is always 1:1 in all analyzed cases. The variant used are summarized in Table 1.

**Table 1** Variants used in the calculations

Pressure angle at normal section	$\alpha$	15...25°
Helix angle at reference circle	$\beta$	0°
Normal module	$m_n$	1...5 mm
Tooth number	$z_1/z_2$	35/35...105/105
Profile shift coefficient	$x_1/x_2$	0/0
Addendum coefficient of the tool	$u_{\text{add}}$	1.25
Tip radius factor of the tool	$r_{\text{add}}$	0.2
Rim thickness coefficient	$S_R$	4...13 × $m_n$ mm
Nominal circum. force at pitchcircle	$F_t$	100...500 N

It is important to note that in this case it is no longer worth relying on the comparison with analytical methods because the chosen boundary conditions radically influence the results. The main reason for this is a strong modifying effect of the selected hubs. Even if you change the normal module, it is obvious that the gears are simply enlarged on a scale, but such a clear procedure cannot be used when the tooth number varies. The theoretical considerations for the effect of the used hub geometry are discussed in more detail in Section 3. Here only specific regulations for the analysis of the impact of the tooth number are presented. The first option for the calculations is to record the rim thickness independently of the tooth number which results in an increasingly thinner rim in relation of the gear hub by increasing the tooth number. As a result of this setup, we can predict the significant dependence of the single stiffness on the tooth number, as proved by the calculations performed. The effect of the tooth number used on single stiffness should be examined by maintaining the proportions of the hubs. This series of calculations no longer comprises the extreme change of the hubs, thus a more comprehensive comparison is possible. The SRX model case of the rim thickness is defined as:

$$SR_9 \approx 9m_z / 35. \quad (1)$$

This connection indicates the notation of dimension [x m] in the abscissa on the diagrams. This approach results the direct dependence of the rim thickness on the normal module for gears with 35 teeth and it allows to be retained the proportion of the deformable rim thickness as a function of the tooth number.

### 3. Hub settings

The problem of comparability of the absolute values of each process has already been mentioned which is caused by the calculation of the deformation of the hubs. Neither the ISO nor the WB calculations consider the exact geometry of the

hub. Furthermore, the deformation of the hub in the calculation of the single stiffness is interpreted only as a function of the profile geometry. The only exception is the "blank factor" of the ISO standard. Therefore, the absolute value of FE results can only be compared with knowledge of the geometry of a given hub. As a result, it is worthwhile carrying out the comparison on the tendency change of the absolute value. The aim is to show the difference in the forecast of the expected single stiffness by using the analytical calculations or the FE method at different rim thicknesses. Even though the deformation of the hubs is taken into account only in a simplified form, the analytical methods represent the relative deformation of the individual teeth well, as they accurately reflect the relative distortion of the teeth and the segment of the gear bodies that is in contact with the teeth. Therefore, if the deflection of the hubs is properly considered when determining the spatial position of the teeth, analytical methods provide a suitable tool for determining the change of connection characteristics in the contact zone. The extra possibilities of the calculations of the deformation provided by the finite element method are of importance in the vibration analysis of the system since it is necessary to represent the specific stiffness of the mesh. During the tests performed in Section 3, the change of single stiffness of a cylindrical gear is exhibited considering the deformation of the hubs for different rim thicknesses. Since the hub itself can be divided into a set of elements whose deformation is determined by the stress at their contact interfaces, it is worth modelling the gears as elements with different rim thicknesses. Thus, if the approximation of deformable elements as a series of springs coupled is accepted, the stiffness change of the gear pairs can be expressed as the change in the stiffness of the modified range of the gears. In the examinations it is useful to consider the relatively small area of the rim for analyzing the single stiffness of the variations of profile geometries since the modifications made will have an effect in this range. This case corresponds to the model SR4 which means that rim thickness has been chosen as the quadruple of the normal module. A further reduction of the rim thickness may influence on the tooth root stress and on the deformation of the teeth. In the model SR4, there is still a safety factor to the borderline case. The maximum thickness of rims has been taken into account during the analyses and it was determined as the model SR13. This position covers shaft diameter capable of conveying the 300 N tangential force with an adequate safety factor for the 35 teeth gears.

#### 4. Results and discussion

The performed impact assessments are summarized in Section 4. The geometries used by FEM are produced with a self-made program. The MATLAB program defines the profile geometry with the modelling of machine kinematics on the base of Litvin's work [34]. Our program allows a direct control of the precision of geometry to avoid singularities. The generated geometry is then converted to Abaqus. The precision of FE mesh quality and of the applied geometry is particularly important for the precise approximation of the deformation at the contact point. The mesh is generated with quadratic quadrilateral elements and the required size of elements to the good convergent results is always controlled based on the size of the analyzed gears. The average mesh size of the contacted teeth is 0.4 % of the whole depth. The remaining areas of gears are meshed with a varied element size depending on the effect on the results. For the simulations is used the reduced integration method. The interaction between the gears is defined as a Hertzian contact. It means that a 0 friction coefficient is applied. The contact formulation is finite sliding. The boundary conditions of finite element models are set based on the analytical methods used for the comparison [1, 2]. The material of gears is always steel.

The deformation results are evaluated by continuously monitoring the obtained stress values. Single stiffness is determined by the load-induced rotation angle of driving gear. For a better overview of the calculation results, Tables 1 to 6 summarizing the variants in the given evaluations are also provided. Fig. 1 shows the general form of the model thus obtained.

The notations applied on Figs. 2 to 13 are below:

- $\Delta c'$  – single stiffness change in %
- FE – finite element method
- ISO – method of ISO 6336-1:2006 [1]

**Table 2** Variants for the calculation of the effect of pressure angle

Pressure angle at normal section	$\alpha$	15; 20; 25°
Normal module	$m_n$	1 mm
Tooth number	$z_1/z_2$	35/35
Rim thickness coefficient	$S_R$	4; 9; $13 \times m_n$ mm
Nominal circum. force at pitch circle	$F_t$	300 N

**Table 3** Variants for the calculation of the effect of module

Pressure angle at normal section	$\alpha$	15; 17; 20; 23; 25°
Normal module	$m_n$	1; 3; 5 mm
Tooth number	$z_1/z_2$	35/35
Rim thickness coefficient	$S_R$	4; 9; $13 \times m_n$ mm
Nominal circum. force at pitch circle	$F_t$	300 N

**Table 4** Variants for the calculation of the effect of load

Pressure angle at normal section	$\alpha$	15; 20; 25°
Normal module	$m_n$	1; 3; 5 mm
Tooth number	$z_1/z_2$	35/35
Rim thickness coefficient	$S_R$	4; 9; $13 \times m_n$ mm
Nominal circum. force at pitch circle	$F_t$	100; 300; 500 N

**Table 5** Variants for the calculation of the effect of rim thickness

Pressure angle at normal section	$\alpha$	15; 20; 25°
Normal module	$m_n$	1; 5 mm
Tooth number	$z_1/z_2$	35/35
Rim thickness coefficient	$S_R$	4... $13 \times m_n$ mm
Nominal circum. force at pitch circle	$F_t$	300 N

**Table 6** Variants for the calculation of the effect of tooth number

Pressure angle at normal section	$\alpha$	15; 20; 25°
Normal module	$m_n$	1; 5 mm

Tooth number	$z_1/z_2$	35/35; 70/70; 105/105
Rim thickness coefficient	$S_R$	4; 9; $13 \times m_n$ mm
Nominal circum. force at pitch circle	<hr/> <hr/>	300 N

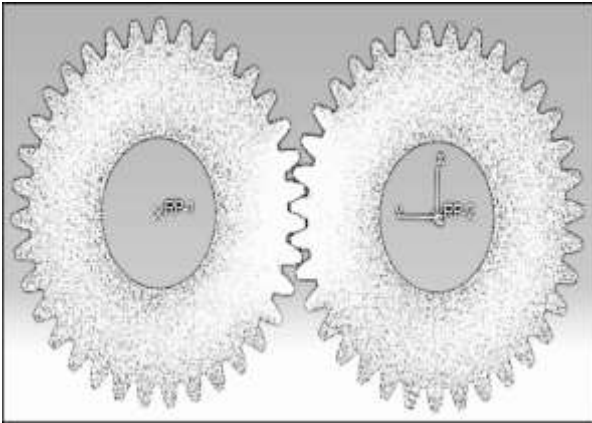


**Fig. 1** Finite element model of meshing pair

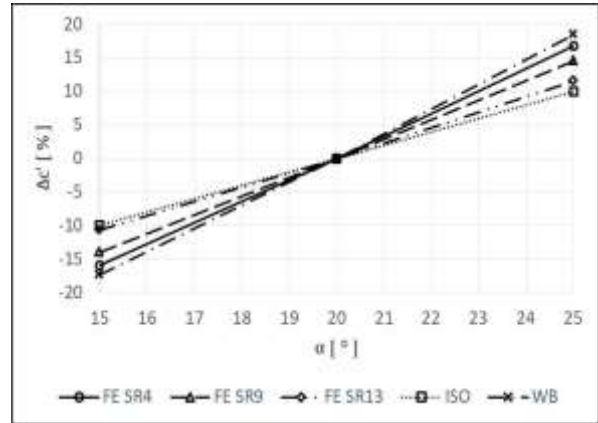


**Fig. 2** Single stiffness changes as a function pressure angle for different rim thicknesses

- WB – method of Weber and Banaschek
- SRX – rim thickness by Eq. (1)
- $zX$  – number of teeth =  $X$  [ - ]
- $mX$  – normal module =  $X$  [mm]
- $FtXN$  –  $X$  [N] tangential load
- $\Delta$  FE SRX - ISO – different between FE with SRXrim thickness and method of ISO 6336-1:2006 [1]

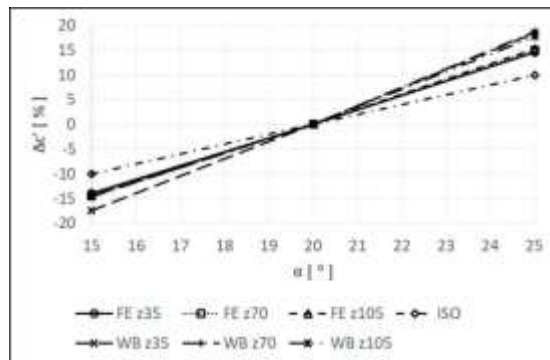


**Fig. 3** Single stiffness changes versus pressure angle for Different tooth number

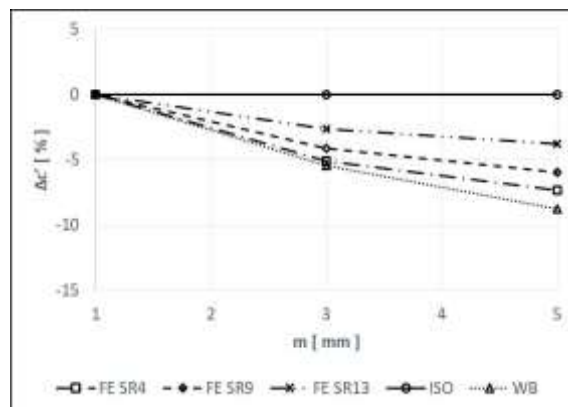


**Fig. 4** Typical single stiffness changes as a function of module

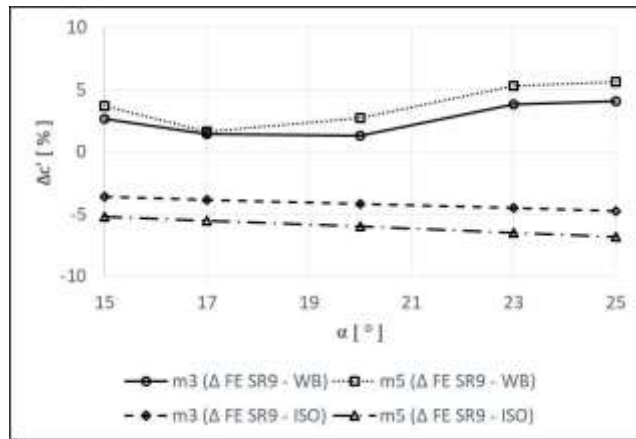


**Fig. 5** Correlation of single stiffness changes by FEM according to ISO and WB methods for different normal

- $\Delta$  FE SRX - WB – different between FE with SRXrim thickness and WB method
- $\Delta$  zX-Y – different between the models with X and Y tooth number.

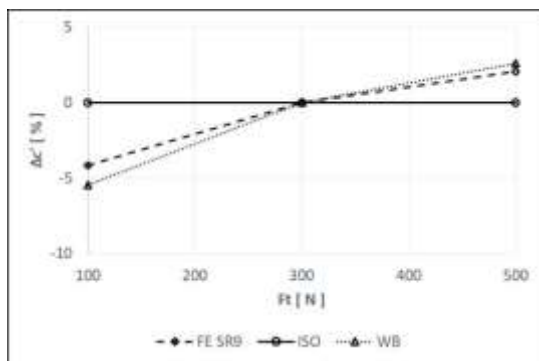


**Fig. 6** Typical single stiffness changes as function of load

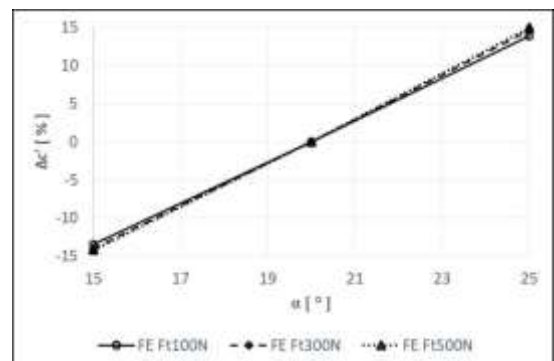


**Fig. 7** Single stiffness changes as a function of pressure angle at different loads

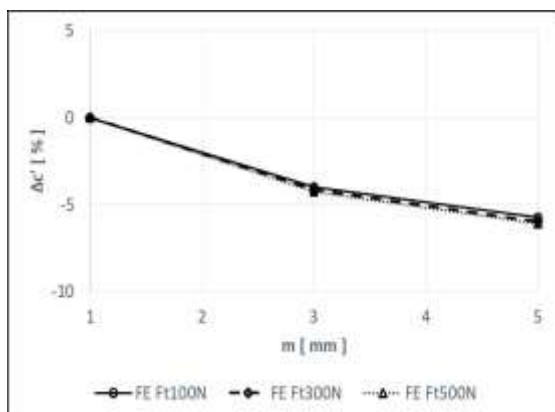


**Fig. 8** Single stiffness changes as a function of normal module at different loads

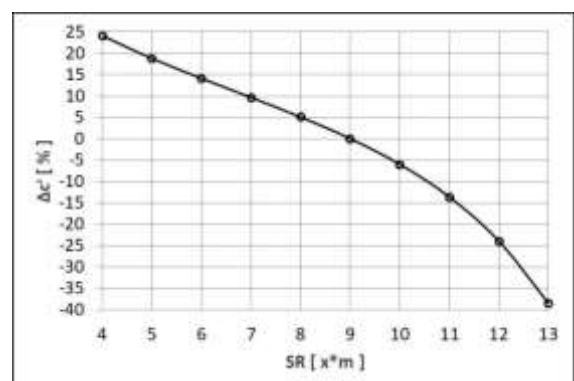


**Fig. 9** Typical single stiffness change as a function of trim thickness



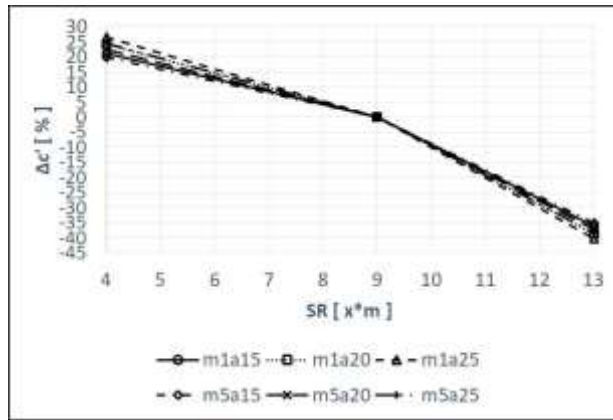


Fig. 10 Single stiffness changes as a function of rim thickness at different pressure angles and modules

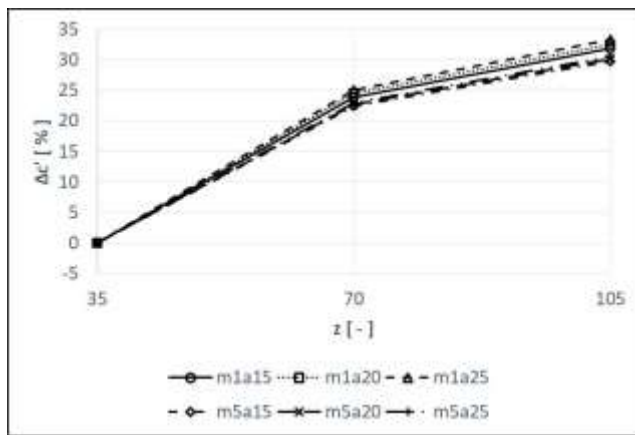


Fig. 11 Single stiffness changes as a function of tooth number at a constant rim thickness

**The change of the single stiffness as a function of the pressure angle**

The calculation results of the gear pairs with 35 teeth are shown in Fig. 2. The deviation of the single stiffness values in the investigated pressure angle range compared to the model SR9 is within the 3.3 % range. This means a difference in stiffness variation of less than 10.6 % between the extremes obtained.

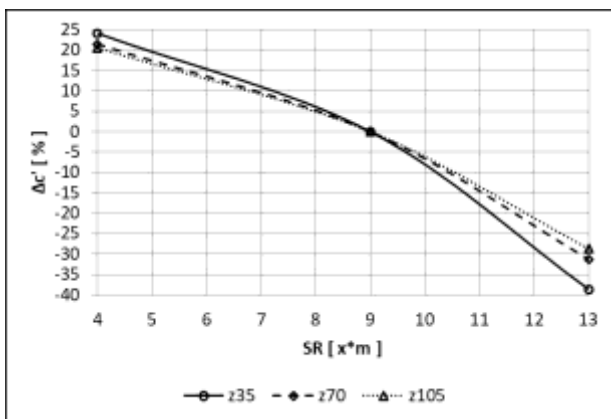


Fig. 12 Single stiffness changes as a function of rim thickness for different tooth numbers

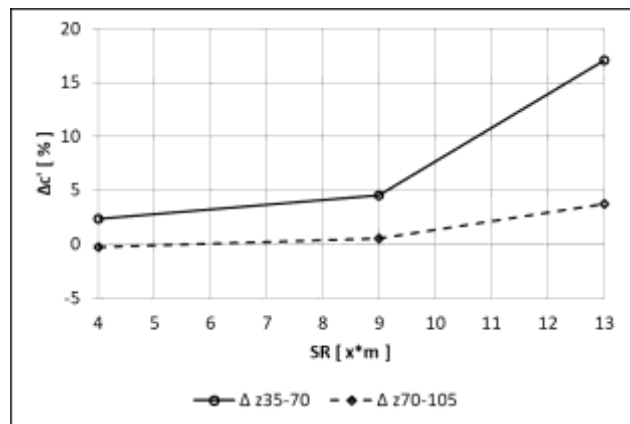


Fig. 13 Single stiffness changes associated with the increase of tooth number

We remark that the slopes of the two extreme cases are very close to the relevant analytical solutions. The models SR13 show a difference of 1.5 % from the ISO results for the selected 20° pressure angle model and, in the extreme cases, show a difference of 2.3 %. The models SR4 are much closer to the results of the WB method. There is a maximum difference of 1.6 % in the 20° profile and 3.0 % in the extreme. In addition to the variants with 35 teeth, it is also worthwhile to examine the pressure angle dependence of the variants with larger tooth numbers. The results in Fig. 3 show the single stiffness changes if the rim thickness of the models corresponds to the normal module multiplied by 9. This means that the gears have a narrowing rim thickness with increasing tooth number in relation to the full gear body. Fig. 3 shows that the finite element results do not exceed the predicted sensitivity by WB even in the model of the 105 tooth number. If the rim thickness of the gears is increased, the curves would be shifted toward the ISO results according to Fig. 2. As a result, we can conclude that the WB calculations typically overestimate the sensitivity of the single stiffness for the pressure angle change. The method described by ISO produces a constant slope in the examined range, which reflects the tendencies of the FE models with large rim thickness.

#### **Single stiffness changes as a function of module**

Fig. 4 shows a typical change of the single stiffness obtained for normal module at different rim thicknesses. To determine this, besides the models SR9, the analysis of the models SR4 and SR13 is required. The differences in the profile angles are summarized in Fig. 5. It is observed that the finite element method shows a decrease in single stiffness by increasing the normal module. In contrast, ISO solutions are insensitive to this parameter. As a result, the finite element method shows -6.8–0 % difference in the examined cases compared to the ISO. The WB method typically overestimates the gradient of the stiffness change. This means a maximum deviation of +5.6 % for the current models. It can be observed that the solutions provided by the finite element method are always located between the two analytical methods. As expected, the significance of the change in normal module to total deformation decreases with increasing rim thickness. Thus, ISO provides a relatively accurate trend for gears with large rim thickness.

#### **Single stiffness changes as a function of load**

The change in the value of single stiffness for the load dependence is illustrated in Fig. 6 for models SR9. Fig. 7 shows the dependence of the single stiffness change on the pressure angle at different loads. The results show less than 1.0 % difference in the stiffness change based on a 20° profile angle. This gives less than 1.8 % deviation between the extreme situations investigated. Fig. 8 represents the dependence on the normal module. The difference in the single stiffness change is less than 0.4 % in these cases. On the base of the calculations performed, it can be stated that the effect of the change in load on the variants investigated is very small for both the chosen pressure angle and the chosen normal module. As a result, the single stiffness change as a function of the applied pressure angle and the normal module can be independent of the magnitude of the load at the variants analyzed. Of course, this does not match the condition of the load independence of the absolute values considered. With respect to the analyzed models SR9, the single stiffness change as a function of load is observed between -5.0 and 2.5 % compared to the obtained values at 300 N tangential load.

**Single stiffness changes as a function of rim thickness** The previous results indicate that the choice of the magnitude of rim thickness has a significant effect on the single stiffness. Fig. 9 depicts a typical single stiffness change as a function of rim thickness. The model SR9 served as a benchmark for the evaluation. The stiffness change shown in Fig. 9 is not independent of the profile geometry used. Fig. 10 illustrates the pressure angle and module dependence on the effect of rim thickness. The results show a single stiffness change between +27 and -40 % relative to models SR9. It is noticeable that the variants with smaller normal modules and larger pressure angles have the most sensitive response to change of the rim thickness. The difference in stiffness change in the extreme cases is in the 6.5% range for models SR4 and in the 5.0 % range for models SR13.

**Single stiffness changes as a function of rim thickness** The importance of hub geometry was already discussed in Section 2. Fig. 11 shows the trend of the single stiffness change of the gear pairs at the same rim thickness. The selected thickness corresponds to the normal module multiplied by 9. The results show an increase in the single stiffness between 22.4 and 25.0 % in the range of variants with 35 and 70 teeth and an increase between 7.4 and 8.3 % in the range of variants with 70 and 105 teeth. This means a change from 29.8 to 33.3 % across the range. According to the conclusions in Section 2, the effect of the tooth number used on single stiffness should be examined by using variants with the same proportion of the hubs. Fig. 12 summarizes the results of the single stiffness change of gear pairs at different tooth numbers versus the rim thickness. Fig. 12 shows a more intensive convergence of the obtained tendencies with increasing tooth number. Fig. 13 illustrates the single stiffness change associated with increasing the tooth number. It can be seen that the use of greater rim thickness cases

results in a growing difference and that the difference is significantly greater for smaller tooth numbers. Accordingly, the change between the variants with 35 and 70 tooth numbers is % in the range SR4-9 and 17.1 % in the range SR9-13. However, the models with 70 and 105 tooth numbers show only 0.5 % difference in the range SR4-9 and 3.7 % in the range SR9-13. In the latter case, a slight decrease can be seen in single stiffness at the models SR4. However, the magnitude of the difference is comparable to the expected accuracy of the calculations.

## 5 Conclusions

By comparing the ISO standard and the WB calculation for the investigated geometric variants, the investigations of the pressure angle, module, and load dependence on the single stiffness reveal parameter sensitivity. The value of the utilized rim thickness has the biggest impact on the correlation rate between the individual solutions. The experiments have demonstrated that, under the considered conditions, the development of the single stiffness as a function of pressure angle and the normal module can be independent of the load magnitude. The importance of the gear body's size has been highlighted by the confirmation of the primary impact of rim thickness. The impact of hub size has also been brought to light through research on how tooth number affects single stiffness. The experiments correctly illustrate how a single stiffness depends on various parameters. The findings show a relationship between the comparability constraints and the sensitivity of each approach to changes in the examined parameters.

## References

- [1] International Organization for Standardization "ISO 6336-1:2006 Calculation of load capacity of spur and helical gears – Part 1: Basic principles, introduction and general influence factors", International Organization for Standardization, Geneva, Switzerland, 2006.
- [2] Weber, C., Banaschek, K. "Formänderung und Profilrücknahme bei gerad- und schrägverzahnten Rädern" (Deformation and tip relief of spur and helical gears), Schriftenreihe Antriebstechnik, Fiedr. Vieweg & Sohn, Braunschweig, Germany, 1953. (in German)
- [3] Lutz, M. "Methoden zur rechnerischen Ermittlung und Optimierung von Tragbildern an Schneckengetrieben" (Methods for the calculation and optimization of contact pattern of worm drives), PhD Thesis, Technische Universität München, 2000. (in German)
- [4] Kagawa, T. "Deflection and Moments Due to a Concentrate Edgeload on a Cantilever Plate of Finite Length", In: 11th Japan National Congress for Applied Mechanics, Tokyo, Japan, 1961.
- [5] Hayashi, K. "Load Distribution on the Contact Line of Helical Gear Teeth: Part 1 Fundamental Concept", Bulletin of JSME, 6(22), pp. 336–343, 1963.
- [6] Schmidt, G. "Berechnung der Wälzpressung schrägverzahnter Stirnräder unter Berücksichtigung der Lastverteilung" (Calculation of contact pressure of helical gears taking into account the load distribution), PhD Thesis, Technische Universität München, 1972. (in German)
- [7] Ma, H., Zeng, J., Feng, R., Pang, X., Wen, B. "An improved analytical method for mesh stiffness calculation of spur gears with tip relief", Mechanism and Machine Theory, 98, pp. 64–80, 2016. <https://doi.org/10.1016/j.mechmachtheory.2015.11.017>
- [8] Gu, X., Velex, P., Sainsot, P., Bruyère, J. "Analytical Investigations on the Mesh Stiffness Function of Solid Narrow Faced Spur and Helical Gears", In: ASME 2015 International Design Engineering Technical Conferences and Computers and Information in Engineering Conference, Boston, MA, USA, 2015, Article Number: V010T11A014. <https://doi.org/10.1115/DETC2015-46061>
- [9] Fernández, A., Iglesias, M., de-Juan, A., García, P., Sancibrián, R., Viadero, F. "Gear transmission dynamic: Effects of tooth profile deviations and support flexibility", Applied Acoustics, 77, pp. 138–149, 2014. <https://doi.org/10.1016/j.apacoust.2013.05.014>
- [10] Chen, Z., Shao, Y. "Mesh stiffness calculation of a spur gear pair with tooth profile modification and tooth root crack", Mechanism and Machine Theory, 62, pp. 63–74, 2013. <https://doi.org/10.1016/j.mechmachtheory.2012.10.012>
- [11] Gerber, H. "Innere dynamische Zusatzkräfte bei Stirnradgetrieben" (Intern dynamic forces of gearboxes with cylindrical gear pairs), PhD Thesis, Technische Universität München, 1984. (in German)
- [12] Cui, L., Liu, T., Huang, J., Wang, H. "Improvement on Meshing Stiffness Algorithms of Gear with Peeling", Symmetry, 11(5), Article Number: 609, 2019. <https://doi.org/10.3390/sym11050609>
- [13] Ma, R., Chen, Y. S. "Bifurcation of multi-freedom gear system with spalling defect", Applied Mathematics and Mechanics, 34(4), pp. 475–488, 2013. <https://doi.org/10.1007/s10483-013-1684-7>

- [14] Saxena, A., Parey, A., Chouksey, M. "Time varying mesh stiffness calculation of spur gear pair considering sliding friction and spalling defects", *Engineering Failure Analysis*, 70, pp. 200–211, 2016. <https://doi.org/10.1016/j.engfailanal.2016.09.003>
- [15] He, S., Cho, S., Singh, R. "Prediction of dynamic friction forces in spur gears using alternate sliding friction formulations", *Journal of Sound and Vibration*, 309(3–5), pp. 843–851, 2008. <https://doi.org/10.1016/j.jsv.2007.06.077>
- [16] Rebbeschi, B., Oswald, F. B., Townsend, D. P. "Measurement of Gear Tooth Dynamic Friction", In: *Seventh International Power Transmission and Gearing Conference*, San Diego, CA, USA, 1996, Article Number: ARL-TR-1165. [online] Available at: <https://core.ac.uk/download/pdf/42775803.pdf> [Accessed: 26 June 2019]
- [17] Ankouni, M., Lubrecht, A. A., Velex, P. "Modelling of damping in lubricated line contacts - Applications to spur gear dynamic simulations", *Proceedings of the Institution of Mechanical Engineers, Part C: Journal of Mechanical Engineering Science*, 230(7–8), pp. 1222–1232, 2016. <https://doi.org/10.1177/0954406216628898>
- [18] Zhang, Y., Wang, Q., Ma, H., Huang, J., Zhao, C. "Dynamic analysis of three-dimensional helical geared rotor system with geometric eccentricity", *Journal of Mechanical Science and Technology*, 27(11), pp. 3231–3242, 2013. <https://doi.org/10.1007/s12206-013-0846-8>
- [19] Wang, Q., Zhang, Y. "A model for analyzing stiffness and stress in a helical gear pair with tooth profile errors", *Journal of Vibration and Control*, 23(2), pp. 272–289, 2017. <https://doi.org/10.1177/1077546315576828>
- [20] Qin, W. J., Guan, C. Y. "An investigation of contact stresses and crack initiation in spur gears based on finite element dynamics analysis", *International Journal of Mechanical Sciences*, 83, pp. 96–103, 2014. <https://doi.org/10.1016/j.ijmecsci.2014.03.035>
- [21] Parker, R., Vijayakar, S. M., Imajo, T. "Non-linear Dynamic Response of a Spur Gear Pair: Modelling and Experimental Comparisons", *Journal of Sound and Vibration*, 237(3), pp. 435–455, 2000. <https://doi.org/10.1006/jsvi.2000.3067>
- [22] Cooley, C., Parker, R. G., Vijayakar, S. M. "An Efficient Finite Element Solution for Gear Dynamics", *IOP Conference Series: Materials Science and Engineering*, 10(1), 2010, Article Number: 012150. <https://doi.org/10.1088/1757-899X/10/1/012150>
- [23] Guilbert, B., Velex, P., Dureisseix, D., Cutuli, P. "Modular hybrid models to simulate the static and dynamic behaviour of high-speed thin-rimmed gears", *Journal of Sound and Vibration*, 438, pp. 353–380, 2019. <https://doi.org/10.1016/j.jsv.2018.09.003>
- [24] Wu, J. S. S., Xu, S. L., Lin, Y. T., Chen, W. H., Lai, Y. L. "3D contact analysis of conjugate spur gears by a complete mating process", *Journal of Mechanical Science and Technology*, 27(12), pp. 3787–3795, 2013. <https://doi.org/10.1007/s12206-013-0923-z>
- [25] Hwang, S. C., Lee, J. H., Lee, D. H., Han, S. H., Lee, K. H. "Contact stress analysis for a pair of mating gears", *Mathematical and Computer Modelling*, 57(1–2), pp. 40–49, 2013. <https://doi.org/10.1016/j.mcm.2011.06.055>
- [26] Li, S. "Effect of addendum on contact strength, bending strength and basic performance parameters of a pair of spur gears", *Mechanism and Machine Theory*, 43(12), pp. 1557–1584, 2008. <https://doi.org/10.1016/j.mechmachtheory.2007.12.010>
- [27] Zhan, J., Fard, M., Jazar, R. "A quasi-static FEM for estimating gear load capacity", *Measurement*, 75, pp. 40–49, 2015. <https://doi.org/10.1016/j.measurement.2015.07.036>